

## HEAVY FLAVOR PHYSICS IN LHCb\*

A. AUGUSTO ALVES JR

on behalf of the LHCb Collaboration

INFN sezione di Roma, Universita' degli Studi di Roma "La Sapienza"  
P. le Aldo Moro, 2, 00185 Roma, Italy

*(Received April 17, 2012)*

This contribution summarises some of the main measurements performed by the LHCb experiment on heavy flavor physics, using data samples recorded during 2010 and 2011 in proton–proton collisions at  $\sqrt{s} = 7$  TeV.

DOI:10.5506/APhysPolB.43.1413

PACS numbers: 13.25.Hw, 14.40.Pq, 14.40.Lb, 14.20.Mr

**1. Introduction**

Measurements of the heavy quark production cross sections in proton–proton collisions test the predictions of quantum chromodynamics (QCD) and dynamics of the colliding partons. In the framework of QCD, the production of heavy bounded  $q\bar{q}$  states (quarkonia states) can be described in two steps. The first one, treatable using perturbative techniques, involves the creation of a  $q\bar{q}$  pair via small-distance interactions. The second step is the evolution into a quarkonium state via the exchange of soft gluons, not treatable perturbatively.

According to non-relativistic QCD (NRQCD) predictions, the probability of a heavy  $q\bar{q}$  pair to evolve into heavy quarkonium is a function of color-singlet (CS) [1, 2] and color-octet (CO) [3] matrix elements. The CS model at leading-order (LO) does not describe the Tevatron data. The better agreement is observed at NLO (next-to-LO) and NNLO (next-to-next-LO).

The CS model at LO does not describe satisfactorily the measured cross section for  $J/\psi$  production at the Tevatron [4]. On the other hand, using the CO model with matrix elements tuned to data, one can obtain a significantly better description of the measured shape and magnitude of the  $J/\psi$  cross section.

---

\* Presented at the Cracow Epiphany Conference on Present and Future of  $B$  Physics, Cracow, Poland, January 9–11, 2012.

Even if recent theoretical studies [5,6] incorporating higher order corrections to the CS models have reduced significantly the discrepancy between measurements and predictions of quarkonium production without including CO matrix elements, the agreement is still not satisfactory. This keeps the discussions about a complete description of quarkonia formation open [7,8].

Furthermore, the discrepancies between the observations and the predicted spectrum of heavy hadrons, calculated using QCD potentials and chiral models [9, 10, 11, 12, 13, 14, 15, 16, 17, 18], makes heavy flavor spectroscopy an active and often controversial field.

This report discusses some of the results of the LHCb experiment on flavor physics production and spectroscopy, presented at Cracow Epiphany Conference of 2012. It was not possible to discuss all presented analysis here. The description of other analyzes can be found in cited references:  $\chi_{c1}$  and  $\chi_{c2}$  production [19,20],  $X(3872)$  mass and cross section measurements [21,22,23],  $B^+$  production [24,25] and  $\Upsilon$  production [26,27].

## 2. The LHCb detector

LHCb is an experiment dedicated to heavy flavor physics at the LHC [28]. Its primary goal is to search for indirect evidence of new physics in CP violation and rare decays of beauty and charm hadrons.

The LHCb detector is a single-arm spectrometer (see Fig. 1) with a forward angular coverage from approximately 10 mrad to 300 (250) mrad in the bending (non-bending) plane, corresponding to a pseudorapidity range of  $2 < \eta < 5$ . In fact, the detector geometry is optimized to cover the region

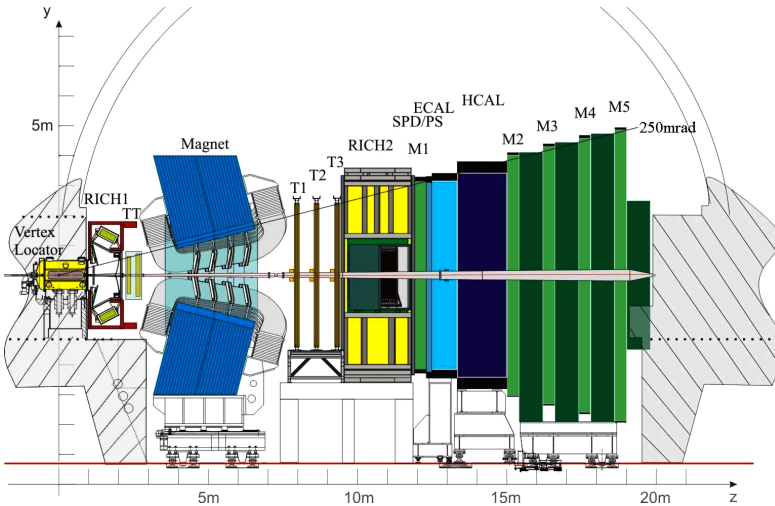


Fig. 1. YZ view of the LHCb detector.

where the  $b\bar{b}$  cross section peaks in such a way that the LHCb detects about 40% of heavy quark hadrons produced in the proton–proton collisions while covering only about 4% of the solid angle.

The spectrometer consists of a vertex locator, a warm dipole magnet, a tracking system, two RICH detectors, a calorimeter system and a muon system. The track momenta are measured to a precision of  $\delta p/p$  between 0.35 and 0.5%. The Ring Imaging Cherenkov Detector (RICH) system provides excellent charged hadron identification in a momentum range 2–100 GeV/ $c$ . The calorimeter system identifies high transverse energy hadron, electron and photon candidates and provides information for the trigger. The muon system provides information for the trigger and muon identification with an efficiency of about 95% for a misidentification rate of about 1–2% for momenta above 10 GeV/ $c$ .

The luminosity for the LHCb experiment can be tuned by changing the beam focus at its interaction point independently from the other interaction points, allowing LHCb to maintain the optimal luminosity in order not to saturate the trigger or to damage the delicate sub-detectors parts. In fact, due to this capability, LHCb was able to keep its luminosity at the constant value of  $3.5 \times 10^{32} \text{ cm}^{-2} \text{ s}^{-1}$  during most of 2011 data taking.

The trigger chain is composed by a first level hardware trigger and two levels of software triggers. LHCb uses hadrons, muons, electrons and photons throughout the trigger chain, maximizing the trigger efficiency on all heavy quark decays and making the experiment sensitive to many different final states.

In 2010 and 2011, the detector recorded about  $1.1 \text{ fb}^{-1}$  integrated luminosity in proton–proton collisions at  $\sqrt{s} = 7 \text{ TeV}$ , with an efficiency of 90% of the luminosity delivered by the Large Hadron Collider (LHC) to LHCb.

### 3. Double $J/\psi$ production

QCD predicts the prompt production of two charmonia states in the same reaction to be an extremely rare effect. The only observation of this phenomenon in hadronic collisions to date was by the NA3 Collaboration, which found evidence of  $J/\psi$  pair production in multi-muon events in pion–platinum interactions at 150 and 280 GeV/ $c$  and in proton–platinum interactions at 400 GeV/ $c$  [29].

Theoretical calculations based on leading order QCD perturbation theory predict that the total cross section of  $J/\psi$  pair production in proton–proton interaction at  $\sqrt{s} = 7 \text{ TeV}$  is equal to  $\sigma(pp \rightarrow J/\psi J/\psi + X) \sim 24.5 \text{ nb}$  [4, 5]. For the  $J/\psi$  rapidity interval  $2.0 < y_{J/\psi} < 4.5$  relevant to the LHCb experiment, the production cross section of  $J/\psi$  pairs is predicted to be 4.15–4.34 nb [30, 31].

In this analysis [32], the  $J/\psi$  is reconstructed through its decay into a pair of muons. The selection starts by forming  $J/\psi \rightarrow \mu^+\mu^-$  candidates using pairs of oppositely-charged tracks identified as muons, each one with a transverse momentum greater than 650 MeV/c and originated from a common vertex.

Selected  $(\mu^-, \mu^+)$  pairs with an invariant mass in the range  $3.0 < m_{\mu^-\mu^+} < 3.2$  GeV/ $c^2$  are paired to form four-muon combinations  $(\mu^-, \mu^+)_1(\mu^-, \mu^+)_2$ . The tracks corresponding to each four-muon candidate are required to be consistent with originating from a common vertex, compatible with one of the reconstructed proton-proton collision vertices. The number of events with two  $J/\psi$  mesons is extracted from the invariant mass distribution of the first dimuon pair in bins of the invariant mass of the second dimuon pair. The background subtracted and efficiency corrected distribution is modeled by a double Crystal Ball function for the signal and an exponential function for the background component. The fit result is shown in Fig. 2. The event yield after the efficiency correction is

$$N_{J/\psi J/\psi}^{\text{corr}} = 672 \pm 129.$$

The total cross section for double  $J/\psi$  production in the range  $2 < y_{J/\psi} < 4.5$  and  $p_T^{J/\psi} < 10$  GeV/c is calculated as

$$\sigma^{J/\psi J/\psi} = \frac{N_{J/\psi J/\psi}^{\text{corr}}}{\mathcal{L} \times \mathcal{B}_{\mu^+\mu^-}^2},$$

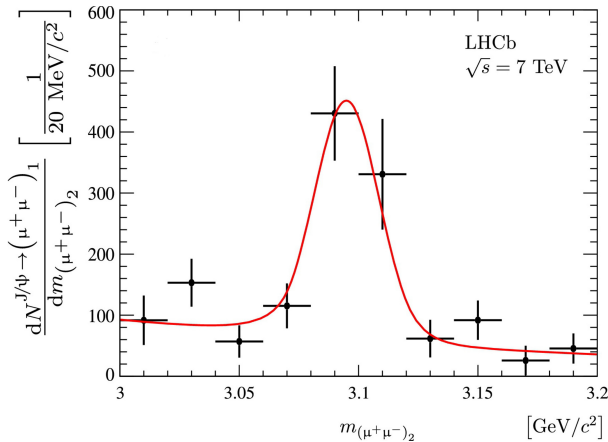


Fig. 2. The efficiency corrected yields of  $(\mu^+, \mu^-)_1$  in bins of  $(\mu^+, \mu^-)_2$  invariant mass. The line represents the fit with a double Crystal Ball function for the signal and an exponential function for the background.

where  $\mathcal{L} = 37.5 \pm 1.3 \text{ pb}^{-1}$  is the integrated luminosity and  $\mathcal{B}_{\mu^+\mu^-} = (5.93 \pm 0.06)\%$  is the  $J/\psi \rightarrow \mu^+\mu^-$  branching ratio [33]. The result is

$$\sigma^{J/\psi J/\psi} = 5.1 \pm 1.0 \pm 1.1 \text{ nb},$$

where the first uncertainty is statistical and the second systematic.

The double  $J/\psi$  production in proton–proton collisions has been observed with a statistical significance in excess of  $6\sigma$ . The data are consistent with the predictions given in Refs. [30, 31].

#### 4. Search for the $X(4140)$ state in $B^+ \rightarrow J/\psi\phi K^+$ decays

The CDF Collaboration has reported a  $3.8\sigma$  evidence for the  $X(4140) \rightarrow J/\psi\phi$  state using data collected in proton–anti-proton collisions at the Tevatron ( $\sqrt{s} = 1.96 \text{ TeV}$ ) [34]. In a preliminary update on the analysis [35], the CDF Collaboration reported  $115 \pm 12$   $B^+ \rightarrow J/\psi\phi K^+$  events and  $19 \pm 6$   $X(4140)$  candidates with a statistical significance of more than  $5\sigma$ . The mass and width were determined to be  $4143.4_{-3.0}^{+2.9} \pm 0.6 \text{ MeV}/c^2$  and  $15.3_{-6.1}^{+10.4} \pm 2.5 \text{ MeV}/c^2$ , respectively. The relative branching ratio was measured to be  $\mathcal{B}(B^+ \rightarrow X(4140)K^+) \times \mathcal{B}(X(4140) \rightarrow J/\psi\phi)/\mathcal{B}(B^+ \rightarrow J/\psi\phi K^+) = 0.149 \pm 0.039 \pm 0.024$ .

Since a charmonium state at this mass is expected to have much larger width because of open flavor decay channels, the decay rate of the  $X(4140) \rightarrow J/\psi\phi$  mode, so near to kinematic threshold, should be small and unobservable. Due to these issues, the CDF’s report rejuvenated the discussions on exotic hadronic states. It was cogitated that the  $X(4140)$  resonance could be a molecular state [36, 37, 38], a tetraquark state [39, 40], a hybrid state [41, 42] or even a rescattering effect [15, 16].

The CDF data also suggested the presence of a second state, referred here as  $X(4274)$  with mass  $4274.4_{-6.4}^{+8.4} \pm 1.9 \text{ MeV}/c^2$  and width  $32.3_{-15.3}^{+21.9} \pm 7.6 \text{ MeV}/c^2$ . The corresponding event yield was  $22 \pm 8$  with  $3.1\sigma$  significance. This observation has also received attention in the literature [43, 44]. On the other hand, the Belle experiment found no evidence for the  $X(4140)$  and  $X(4274)$  states [45, 46].

The LHCb analysis [47, 48] starts reconstructing a  $B^+$  candidate as five-track  $(\mu^+\mu^-K^+K^-K^+)$  vertex using well reconstructed and identified muons and kaons candidates. The  $B^+$  candidates are required to have  $p_T > 4.0 \text{ GeV}/c$  and a decay time of at least  $0.25 \text{ ps}$ . The invariant mass of the  $(\mu^+\mu^-K^+K^-K^+)$  combination is evaluated after the muon pair is constrained to the  $J/\psi$  mass, and all final state particles are constrained to a common vertex. Further background suppression is provided using the likelihood ratio discriminator method.

The  $B^+ \rightarrow J/\psi\phi K^+$  invariant mass distribution, with at least one  $K^+K^-$  combination having an invariant mass within  $\pm 15 \text{ MeV}/c^2$  of the nominal  $\phi$  mass was fitted by a Gaussian and a quadratic function resulting in  $346 \pm 20$   $B^+$  events with a mass resolution of  $5.2 \pm 0.3 \text{ MeV}/c^2$ .

The  $X(4140)$  state was searched selecting events within  $\pm 15 \text{ MeV}/c^2$  of the  $\phi$  mass. Figure 3 shows the mass difference  $M(J/\psi\phi) - M(J/\psi)$  distribution without  $J/\psi$  or  $\phi$  mass constraints. No narrow structure is observed near the threshold. The fit results are  $N_{X(4140)}^{(a)} = 6.9 \pm 4.9$  or  $N_{X(4140)}^{(b)} = 0.6 \pm 7.1$  depending on the background shape used.

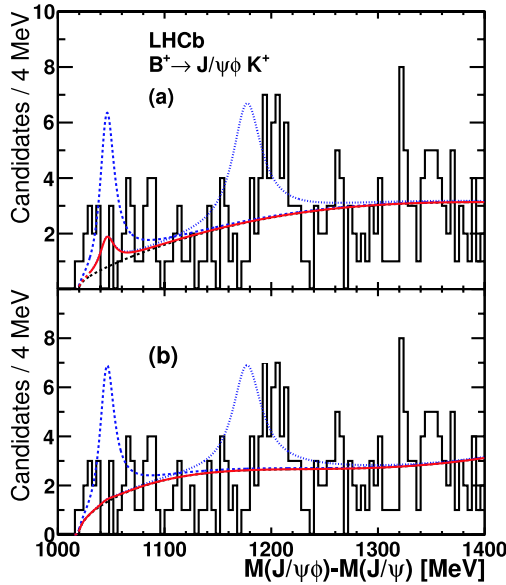


Fig. 3. Distribution of the mass difference  $M(J/\psi\phi) - M(J/\psi)$ . The fit of  $X(4140)$  signal on top of a smooth background is superimposed (solid/red line). The dashed/blue (dotted/blue) line on top illustrates the expected  $X(4140)$  ( $X(4274)$ ) signal yield from the CDF measurement. The top and bottom plots differ by the background function (dashed black line) used in the fit: (a) an background efficiency-corrected three-body phase-space; (b) background a efficiency-corrected quadratic function.

The CDF's fit model was used to quantify the compatibility of the two measurements and considering the LHCb  $B^+ \rightarrow J/\psi\phi K^+$  yield, the efficiency ratio, and the CDF value for  $\mathcal{B}(B^+ \rightarrow X(4140)K^+)/\mathcal{B}(B^+ \rightarrow J/\psi\phi K^+)$ , one concludes that LHCb should have observed  $35 \pm 9 \pm 6$  events, where the first uncertainty is statistical from the CDF data and the second includes both the CDF and LHCb systematic uncertainties. The LHCb

results disagree with the CDF observation by  $2.4\text{--}2.7\sigma$ . In the case of the  $X(4274)$  candidate, the same procedure predicts that LHCb should have observed  $53 \pm 19$   $X(4274)$  candidates. The final analysis results are the upper limits at 90% C.L.

$$\frac{\mathcal{B}(B^+ \rightarrow X(4140)K^+) \times \mathcal{B}(X(4140) \rightarrow J/\psi\phi)}{\mathcal{B}(B^+ \rightarrow J/\psi\phi K^+)} < 0.07,$$

$$\frac{\mathcal{B}(B^+ \rightarrow X(4274)K^+) \times \mathcal{B}(X(4274) \rightarrow J/\psi\phi)}{\mathcal{B}(B^+ \rightarrow J/\psi\phi K^+)} < 0.08.$$

### 5. First observation of $B_c^+ \rightarrow J/\psi\pi^+\pi^-\pi^+$

The  $B_c^+$  meson is the ground state of the  $\bar{b}c$  system and due to its heavy quarks composition, the  $B_c^+$  production rates are about three orders of magnitude smaller compared to the heavy-light  $B$  mesons ( $B_u^+$ ,  $B_d^0$  and  $B_s^0$ ).

The  $B_c^+$  was discovered by the CDF experiment in a semileptonic decay,  $B_c^+ \rightarrow J/\psi l^+ \nu X$  [49] and only one hadronic decay mode has been observed so far,  $B_c^+ \rightarrow J/\psi\pi^+$ , and used by CDF [50] and D0 [51] to measure  $B_c^+$  mass.

The LHCb observed the new hadronic decay mode  $B_c^+ \rightarrow J/\psi\pi^+\pi^-\pi^+$  and measured its branching ratio relatively to  $B_c^+ \rightarrow J/\psi\pi^+$  [52]. Even if the branching ratio for the  $B_c^+ \rightarrow J/\psi\pi^+\pi^-\pi^+$  mode is expected to be 1.5–2.3 times higher than for  $B_c^+ \rightarrow J/\psi\pi^+$  [53, 54], the need to reconstruct more pions in the final state makes more difficult to observe.

The analysis was performed in a data sample of approximately  $303 \text{ pb}^{-1}$  of proton–proton collisions. The decays modes of interest have been reconstructed using good quality and well identified tracks. The final background reduction was performed using signal-to-background likelihood-ratio discrimination techniques. For a detailed description of the selection criteria see [52]. The LHCb analysis result is

$$\mathcal{B}(B_c^+ \rightarrow J/\psi\pi^+\pi^-\pi^+) / \mathcal{B}(B_c^+ \rightarrow J/\psi\pi^+) = 3.0 \pm 0.6 \pm 0.4,$$

where the first uncertainty is statistical and the second systematic (Fig. 4). The result was compared to theoretical predictions. The prediction by Rakitin and Koshkarev, using no-recoil approximation in  $B_c^+ \rightarrow J/\psi W^{+*}$ , is  $\mathcal{B}(B_c^+ \rightarrow J/\psi\pi^+\pi^-\pi^+) / \mathcal{B}(B_c^+ \rightarrow J/\psi\pi^+) = 1.5$  [53], while Likhoded and Luchinsky used three different approaches to predict the form factors and obtained  $\mathcal{B}(B_c^+ \rightarrow J/\psi\pi^+\pi^-\pi^+) / \mathcal{B}(B_c^+ \rightarrow J/\psi\pi^+) = 2.0, 1.9$  and  $2.3$ , respectively [54].

Taking into consideration experimental uncertainties, one can conclude that the lower value, predicted by Rakitin and Koshkarev, is disfavored at about  $2\sigma$ .

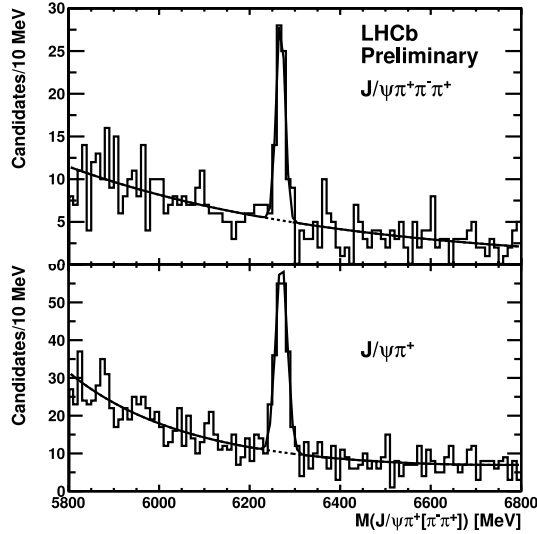


Fig. 4. The fit of  $B_c^+ \rightarrow J/\psi \pi^+ \pi^- \pi^+$  (top) and  $B_c^+ \rightarrow J/\psi \pi^+$  (bottom) signals assumed to be Gaussian on top of a polynomial of first (top) or second (bottom) degree taken to an exponent. The maximum likelihood fits were performed to both distributions with  $2.5 \text{ MeV}/c^2$  bins.

## 6. Orbitally excited $B_{(s)}^{**}$ mesons

The properties of the excited  $B$  mesons containing a light quark ( $B^+$ ,  $B^0$ ,  $B_s^0$ ) are predicted by Heavy Quark Effective Theory (HQET) in the limit of infinite  $b$ -quark mass [13, 55, 56]. These are collectively referred as orbitally excited  $B$  states and labeled as  $B_{(s)}^{**}$ .

The peaks corresponding to decays of these resonances into either  $Bh$  or  $B^*h$  final states ( $h = \pi^\pm, K^\pm$ ) can be identified by analyzing the  $Bh$  invariant mass spectrum. In the case of  $B_{(s)}^{**}$  transitions into  $B^*h$ , the corresponding peak is shifted by  $45.78 \pm 0.35 \text{ MeV}/c^2$ , once the soft photon from  $B^* \rightarrow \gamma B$  is not reconstructed.

This analysis [57] was performed on a  $\sqrt{s} = 7 \text{ TeV}$  proton–proton collisions data sample with  $336 \text{ pb}^{-1}$  of integrated luminosity collected by the LHCb detector between May and July 2011. The analysis starts by reconstructing the  $B^+$  decays into  $\{J/\psi K^+, \bar{D}^0 \pi^+, \bar{D}^0 \pi^+ \pi^- \pi^+\}$  and the  $B^0$  decays into  $\{J/\psi K^*(892), D^- \pi^+, D^- \pi^+ \pi^- \pi^+\}$ . Subsequently, the  $B$  candidates are combined with well reconstructed and identified  $\pi^\pm$  and  $K^\pm$  tracks originated from the same primary vertex.



The signals of excited  $B$  states are expected to appear as peaks above a combinatorial background in the distribution of the  $Q$  variable, defined by  $Q = m_{Bh} - m_B - m_h$ , where  $m_h$  is the nominal mass of the pion.  $m_{Bh}$  and  $m_B$  are the invariant masses of the  $Bh$  combination and  $B$  candidate, respectively.

In the distribution of the  $Q$  variable corresponding to  $B^+K^-$  combinations, LHCb observed two distinct narrow peaks at  $Q$  values close to 10 MeV/ $c^2$  and 67 MeV/ $c^2$  and that are consistent with the  $B_{s1}^0$  and  $B_{s2}^{*0}$  decays (Fig. 5). In the  $Q$  distributions corresponding to the  $B^0\pi$  and  $B^+\pi$ , LHCb observed the three peaks corresponding to the transitions  $B_1 \rightarrow B^*\pi$ ,  $B_2^* \rightarrow B^*\pi$  and  $B_2^* \rightarrow B\pi$ . The interested reader can find further details on the event selection and fit functions and procedure in the reference [57].

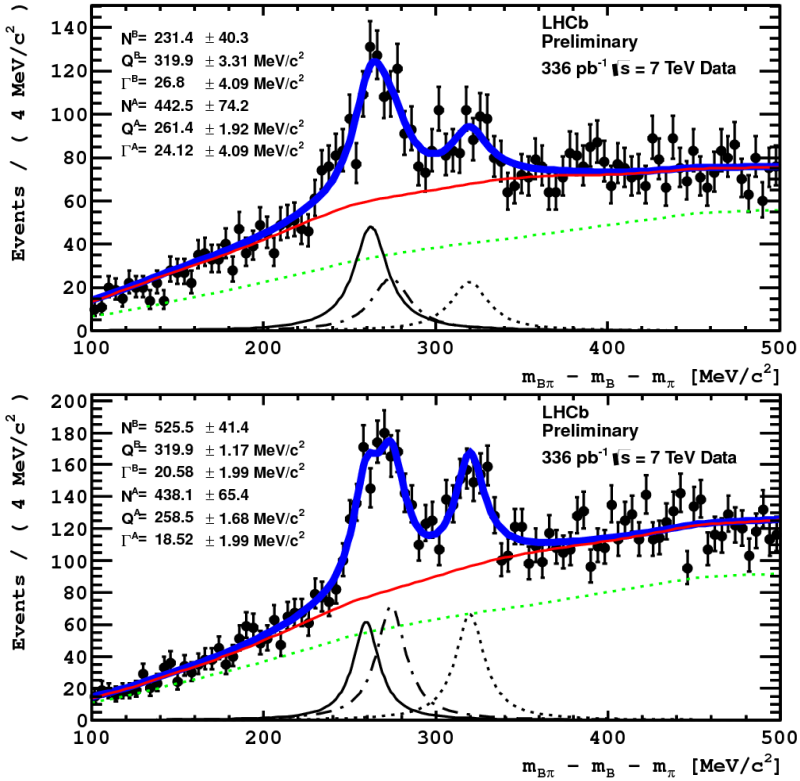


Fig. 5. The fit to the  $Q$  distributions of  $B\pi$  system. In both data plots the total fit functions are shown as thick black (blue) lines. The different components are shown as: light grey (green) for combinatorial background; dark grey (red) for sum of combinatorial background and associated production; black solid  $B_1 \rightarrow B^*\pi$ ; black dot-dashed for  $B_2^* \rightarrow B^*\pi$ ; black dotted for  $B_2^* \rightarrow B\pi$ .

Finally, the measured  $Q$  values were translated into masses by adding the PDG masses of the decay's product mesons. In the case of the  $B_{(s)1}^0$  states, was used the  $B^* - B$  PDG mass difference

$$\begin{aligned} M_{B_{s1}^0} &= (5828.99 \pm 0.08_{\text{stat}} \pm 0.13_{\text{syst}} \pm 0.45_{\text{syst}}^{B \text{ mass}}) \text{ MeV}/c^2, \\ M_{B_{s2}^{*0}} &= (5839.67 \pm 0.13_{\text{stat}} \pm 0.17_{\text{syst}} \pm 0.29_{\text{syst}}^{B \text{ mass}}) \text{ MeV}/c^2, \\ M_{B_1^0} &= (5724.1 \pm 1.7_{\text{stat}} \pm 2.0_{\text{syst}} \pm 0.5_{\text{syst}}^{B \text{ mass}}) \text{ MeV}/c^2, \\ M_{B_1^+} &= (5726.3 \pm 1.9_{\text{stat}} \pm 3.0_{\text{syst}} \pm 0.5_{\text{syst}}^{B \text{ mass}}) \text{ MeV}/c^2, \\ M_{B_2^{*0}} &= (5738.6 \pm 1.2_{\text{stat}} \pm 1.2_{\text{syst}} \pm 0.3_{\text{syst}}^{B \text{ mass}}) \text{ MeV}/c^2, \\ M_{B_2^{*+}} &= (5739.0 \pm 3.3_{\text{stat}} \pm 1.6_{\text{syst}} \pm 0.3_{\text{syst}}^{B \text{ mass}}) \text{ MeV}/c^2. \end{aligned}$$

All measured masses are in good agreement with the theoretical predictions [13, 55, 56]. The masses of the  $B_1^+$  and  $B_2^{*+}$  mesons were measured for the first time and are consistent with those of the isospin partners.

## 7. $\Omega_b$ and $\Xi_b$ mass measurements at LHCb

The mass measurement of the  $\Omega_b$  is particularly interesting, due to the discrepancy between CDF and D0 in the value of measured mass. Indeed, D0 Collaboration reported [58]  $M(\Omega_b) = 6165 \pm 10 \pm 13 \text{ MeV}/c^2$ , while the CDF Collaboration [59] measured  $M(\Omega_b) = 6054.4 \pm 6.8 \pm 0.9 \text{ MeV}/c^2$ , implying that the difference between these two measurements,  $111 \pm 12 \pm 13 \text{ MeV}/c^2$ , represents a discrepancy higher than  $6\sigma$ . The  $\Xi_b$  particle was also observed at the Tevatron [59, 60, 61].

The analysis [62] was performed on a data sample corresponding to integrated luminosity of  $0.62 \text{ fb}^{-1}$  proton-proton collisions at a center-of-mass energy of  $\sqrt{s} = 7 \text{ TeV}$  and recorded between March and August 2011. The  $\Omega_b$  and  $\Xi_b$  baryons were reconstructed in the following decays modes

$$\begin{aligned} \Xi_b^- &\rightarrow (J/\psi \rightarrow \mu^+ \mu^-) (\Xi^- \rightarrow (\Lambda^0 \rightarrow p \pi^-) \pi^-), \\ \Omega_b^- &\rightarrow (J/\psi \rightarrow \mu^+ \mu^-) (\Omega^- \rightarrow (\Lambda^0 \rightarrow p \pi^-) K^-), \end{aligned}$$

using well reconstructed and identified tracks. Only candidates with a life time greater than  $0.3 \text{ ps}$  have been kept. The detailed description of the whole selection criteria is documented in [62].

The  $\Omega_b$  and  $\Xi_b$  masses have been measured by LHCb to be

$$\begin{aligned} M(\Xi_b) &= 5796.5 \pm 1.2 \pm 1.2 \text{ MeV}/c^2, \\ M(\Omega_b) &= 6050.3 \pm 4.5 \pm 2.2 \text{ MeV}/c^2. \end{aligned} \tag{1}$$

The corresponding fits are showed in Fig. 6. The  $\Xi_b$  result is in good agreement with the world average. The  $\Omega_b$  result is in good agreement with CDF [59] measurement but not with the measurement from D0 [58]. Furthermore, the combination of the LHCb and the CDF  $\Omega_b$  results are in large discrepancy ( $> 6\sigma$ ) with the D0 result.

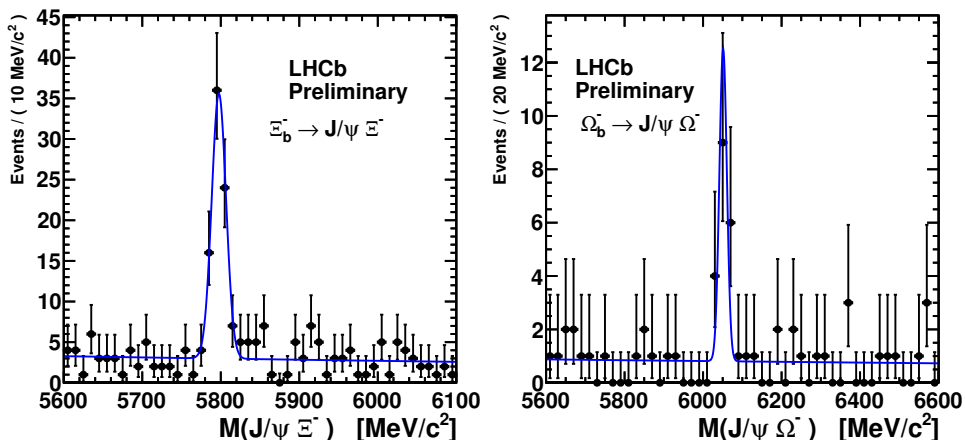


Fig. 6. Invariant mass distributions of  $\Xi_b^- \rightarrow J/\psi \Xi^-$  (left) and  $\Omega_b^- \rightarrow J/\psi \Omega^-$  (right).

## 8. Conclusions

A selection of results on heavy flavor production and spectroscopy at the LHCb detector have been summarized. Many new results are expected from the analysis of the full  $1.1 \text{ fb}^{-1}$  2011 dataset and as well from the new studies currently on-going.

The LHCb experiment is in a privileged position to explore the production mechanisms and spectra of states, delivering competitive results in the heavy flavors sector, in a unique rapidity range.

## REFERENCES

- [1] E.L. Berger, D. Jones, *Phys. Rev.* **D23**, 1521 (1981).
- [2] R. Baier, R. Rückl, *Phys. Lett.* **B102**, 364 (1981).
- [3] E. Braaten, S. Fleming, *Phys. Rev. Lett.* **74**, 3327 (1995).
- [4] CDF Collaboration, *Phys. Rev. Lett.* **69**, 3704 (1992).
- [5] N. Brambilla, X. Garcia i Tormo, J. Soto, A. Vairo, *Phys. Rev.* **D75**, 074014 (2007) [arXiv:hep-ph/0702079].

- [6] P. Artoisenet, J.P. Lansberg, F. Maltoni, *Phys. Lett.* **B653**, 60 (2007) [arXiv:hep-ph/0703129].
- [7] J.M. Campbell, F. Maltoni, F. Tramontano, *Phys. Rev. Lett.* **98**, 252002 (2007) [arXiv:hep-ph/0703113].
- [8] P. Artoisenet, *AIP Conf. Proc.* **1038**, 55 (2008).
- [9] G.T. Bodwin, E. Braaten, G.P. Lepage, *Phys. Rev.* **D51**, 1125 (1995) [arXiv:hep-ph/9407339].
- [10] S. Godfrey, N. Isgur, *Phys. Rev.* **D32**, 189 (1985).
- [11] S. Godfrey, R. Kokoski, *Phys. Rev.* **D43**, 1679 (1991).
- [12] N. Isgur, M.B. Wise, *Phys. Rev. Lett.* **66**, 1130 (1991).
- [13] M. Di Pierro, E. Eichten, *Phys. Rev.* **D64**, 114004 (2001).
- [14] T. Matsuki, T. Morii, K. Sudoh, *Prog. Theor. Phys.* **117**, 1077 (2007).
- [15] BaBar Collaboration, *Phys. Rev. Lett.* **90**, 242001 (2003).
- [16] CLEO Collaboration, *Phys. Rev.* **D68**, 032002 (2003).
- [17] Belle Collaboration, *Phys. Rev. Lett.* **92**, 012002 (2004).
- [18] BaBar Collaboration, *Phys. Rev.* **D69**, 031101 (2004).
- [19] LHCb Collaboration, LHCb-CONF-2011-020.
- [20] LHCb Collaboration, arXiv:1202.1080 [hep-ex].
- [21] LHCb Collaboration, LHCb-CONF-2011-043.
- [22] LHCb Collaboration, LHCb-ANA-2011-030.
- [23] LHCb Collaboration, arXiv:1112.5310 [hep-ex].
- [24] LHCb Collaboration, LHCb-CONF-2011-033.
- [25] LHCb Collaboration, *J. High Energy Phys.* **04**, 93 (2012) [arXiv:1202.4812 [hep-ex]].
- [26] LHCb Collaboration, LHCb-CONF-2011-016.
- [27] The LHCb Collaboration, arXiv:1202.6579 [hep-ex].
- [28] LHCb Collaboration, *JINST* **3**, S08005 (2008).
- [29] NA3 Collaboration, *Phys. Lett.* **B114**, 457 (1982).
- [30] C.-F. Qiao, L.-P. Sun, P. Sun, *J. Phys. G: Nucl. Part. Phys.* **37**, 075019 (2010).
- [31] A. Berezhnoy, A. Likhoded, A. Luchinsky, A. Novoselov, *Phys. Rev.* **D84**, 094023 (2011) [arXiv:1101.5881v3 [hep-ph]].
- [32] LHCb Collaboration, *Phys. Lett.* **B707**, 52 (2012).
- [33] K. Nakamura *et al.* [Particle Data Group], *J. Phys. G* **37**, 075021 (2010).
- [34] CDF Collaboration, *Phys. Rev. Lett.* **102**, 242002 (2009).
- [35] CDF Collaboration, arXiv:1101.6058 [hep-ex].
- [36] Z.-G. Wang, Z.-C. Liu, X.-H. Zhang, *Eur. Phys. J.* **C64**, 373 (2009).
- [37] R.M. Albuquerque, M.E. Bracco, M. Nielsen, *Phys. Lett.* **B678**, 186 (2009).
- [38] J.-R. Zhang, M.-Q. Huang, *J. Phys. G: Nucl. Part. Phys.* **37**, 025005 (2010).

- [39] F. Stancu, *J. Phys. G: Nucl. Part. Phys.* **37**, 075017 (2010).
- [40] N.V. Drenska, R. Faccini, A.D. Polosa, *Phys. Rev.* **D79**, 077502 (2009).
- [41] N. Mahajan, *Phys. Lett.* **B679**, 228 (2009).
- [42] Z.-G. Wang, *Eur. Phys. J.* **C63**, 115 (2009).
- [43] X. Liu, *Phys. Lett.* **B680**, 137 (2009).
- [44] S.I. Finazzo, M. Nielsen, X. Liu, *Phys. Lett.* **B701**, 101 (2011).
- [45] C.P. Shen *et al.* [Belle Collaboration], *Phys. Rev. Lett.* **104**, 112004 (2010).
- [46] J. Brodzicka, Heavy Flavour Spectroscopy in: Lepton Photon 2009 (LP09) Vol., DESY-PROC-2010-04, 2010.
- [47] LHCb Collaboration, [arXiv:1202.5087v1 \[hep-ex\]](#).
- [48] LHCb Collaboration, LHCb-CONF-2011-045.
- [49] F. Abe *et al.* [CDF Collaboration], *Phys. Rev. Lett.* **81**, 2432 (1998) [[arXiv:hep-ex/9805034](#)].
- [50] T. Aaltonen *et al.* [CDF Collaboration], *Phys. Rev. Lett.* **100**, 182002 (2008) [[arXiv:0712.1506 \[hep-ex\]](#)].
- [51] V.M. Abazov *et al.* [D0 Collaboration], *Phys. Rev. Lett.* **101**, 012001 (2008) [[arXiv:0802.4258 \[hep-ex\]](#)].
- [52] LHCb Collaboration, LHCb-CONF-2011-040.
- [53] A. Rakitin, S. Koshkarev, *Phys. Rev.* **D81**, 014005 (2010) [[arXiv:0911.3287 \[hep-ph\]](#)].
- [54] A.K. Likhoded, A.V. Luchinsky, *Phys. Rev.* **D81**, 014015 (2010) [[arXiv:0910.3089 \[hep-ph\]](#)].
- [55] E.J. Eichten, C.T. Hill, C. Quigg, *Phys. Rev. Lett.* **71**, 4116 (1993).
- [56] A.F. Falk, T. Mehen, *Phys. Rev.* **D53**, 231 (1996).
- [57] LHCb Collaboration, LHCb-CONF-2011-053.
- [58] D0 Collaboration, *Phys. Rev. Lett.* **101**, 232002 (2008).
- [59] CDF Collaboration, *Phys. Rev.* **D80**, 072003 (2009).
- [60] CDF Collaboration, *Phys. Rev. Lett.* **99**, 052002 (2007).
- [61] D0 Collaboration, *Phys. Rev. Lett.* **99**, 052001 (2007).
- [62] LHCb Collaboration, LHCb-CONF-2011-060.